Role of Inflammation and Insulin Resistance in Endothelial Progenitor Cell Dysfunction

Cyrus V. Desouza,[1,2] Frederick G. Hamel,[1,2] Keshore Bidasee,[1] and Kelly O'Connell[1,2]

OBJECTIVE—Endothelial progenitor cells (EPCs) are decreased in number and function in type 2 diabetes. Mechanisms by which this dysfunction occurs are largely unknown. We tested the hypothesis that a chronic inflammatory environment leads to insulin signaling defects in EPCs and thereby reduces their survival. Modifying EPCs by a knockdown of nuclear factor-κB (NF-κB) can reverse the insulin signaling defects, improve EPC survival, and decrease neointimal hyperplasia in Zucker fatty rats postangioplasty.

RESEARCH DESIGN AND METHODS—EPCs from Zucker fatty insulin-resistant rats were cultured and exposed to tumor necrosis factor-α (TNF-α). Insulin signaling defects and apoptosis were measured in the presence and absence of an NF-κB inhibitor, BAY11. Then, EPCs were modified by a knockdown of NF-κB (RelA) and exposed to TNF-α. For in vivo experiments, Zucker fatty rats were given modified EPCs post–carotid angioplasty. Tracking of EPCs was done at various time points, and neointimal hyperplasia was measured 3 weeks later.

RESULTS—Insulin signaling as measured by the phosphorylated–to–total AKT ratio was reduced by 56% in EPCs exposed to TNF-α. Apoptosis was increased by 71%. These defects were reversed by pretreatment with an NF-κB inhibitor, BAY11. Modified EPCs exposed to TNF-α showed a lesser reduction (RelA 20%) in insulin-stimulated AKT phosphorylation versus a 55% reduction in unmodified EPCs. Apoptosis was 41% decreased for RelA knockdown EPCs. Noeintimal hyperplasia postangioplasty was significantly less in rats receiving modified EPCs than in controls (intima-to-media ratio 0.58 vs. 1.62).

CONCLUSIONS—In conclusion, we have shown that insulin signaling and EPC survival is impaired in Zucker fatty insulin resistant rats. For the first time, we have shown that this defect can be significantly ameliorated by a knockdown of NF-κB and that these EPCs given to Zucker fatty rats decrease neointimal hyperplasia post–carotid angioplasty. ***Diabetes*** **60:1286–1294, 2011**

Diabetes is at epidemic proportions in the U.S. Insulin resistance without overt diabetes is even more prevalent, with over 25% of the population reported to have several components of the insulin resistance syndrome. The insulin resistance syndrome is associated with hyperinsulinemia, obesity, dyslipoproteinemia, hypertension, and abnormalities of several nontraditional risk factors such as endothelial dysfunction, abnormal fibrinolysis, and inflammation (1,2). Insulin resistance, even in the absence of other traditional cardiovascular risk factors, is associated with endothelial dysfunction in the peripheral and coronary arteries (3). A common complication in patients with diabetes and insulin resistance is restenosis after angioplasty and stent placement. Studies have shown that insulin levels are the best predictor of neointimal proliferation post–angioplasty and stent placement even in patients without diabetes (4,5).

Growing evidence over recent years supports a potential role for cytokine-associated, subacute inflammation in the pathogenesis of insulin resistance and type 2 diabetes (6). Insulin resistance (with or without hyperglycemia), dyslipidemia, and hypertension all increase risk for atherosclerosis, which is itself increasingly thought to be a disease of chronic subacute inflammation (7,8). These interrelationships suggest that inflammation may be the basis of a "common soil" involved in the pathogenesis of both type 2 diabetes and atherosclerosis.

Recent studies suggest that a state of chronic, subacute inflammation—specifically mediated by nuclear factor-κB (NF-κB), c-jun NH_2-terminal kinase, or P38 mitogen-activated protein kinase (MAPK) pathways—might both be involved in the pathogenesis of insulin resistance and provide new targets for its reversal (9–15). Inflammatory cytokines like tumor necrosis factor-α (TNF-α) have been shown to reduce insulin signaling by decreasing insulin receptor substrate (IRS)-1 tyrosine phosphorylation, phosphatidylinositol 3-kinase (PI3K), and AKT activity. These alterations in insulin signaling can lead to increased apoptosis and impaired wound healing.

Endothelial progenitor cells (EPCs) are circulating cells with the ability to differentiate into mature endothelium and take part in endothelial repair and maintenance. A decrease in the number and function of EPCs has been associated with a large number of risk factors for atherosclerosis (16,17). Several studies show that circulating EPCs are decreased in patients with diabetes (18,19). EPCs from diabetic patients display functional impairments, such as reduced proliferation, adhesion, migration, and incorporation into tubular structures (20,21). Decreased number of circulating EPCs has been reported in patients with the insulin resistance syndrome, negatively correlating with homeostasis model assessment of insulin resistance (22). Studies looking at the effects of EPC dysfunction in diabetes on endothelial regrowth and neointimal hyperplasia after vessel injury are very few. One study showed that reendothelialization was significantly reduced in nude nondiabetic mice injected with EPCs from diabetic mice when compared with mice injected with normal EPCs (23,24). However, very little is known about the mechanisms that might lead to the inability of EPCs in an inflammatory, insulin-resistant environment, to induce reendothelialization and decrease neointimal hyperplasia. The inability of EPCs to respond adequately to insulin may result in dysfunction in the setting of insulin-resistant

From the [1]University of Nebraska Medical Center, Omaha, Nebraska; and the [2]Omaha Veterans Affairs Medical Center, Omaha, Nebraska.
Corresponding author: Cyrus V. Desouza, cdesouza@unmc.edu.
Received 23 June 2010 and accepted 12 January 2011.
DOI: 10.2337/db10-0875
This article contains Supplementary Data online at http://diabetes.diabetesjournals.org/lookup/suppl/doi:10.2337/db10-0875/-/DC1.

states and ultimately lead to increased neointimal hyperplasia postangioplasty.

In this article, we test the hypothesis that cytokines present in a chronic inflammatory environment lead to insulin signaling defects in EPCs and thereby reduce their survival. We also test the hypothesis that modifying EPCs by a knockdown of NF-κB can reverse the insulin signaling defects in EPCs and that an infusion of these modified EPCs decreases neointimal hyperplasia postangioplasty in a rat model of insulin resistance.

RESEARCH DESIGN AND METHODS

The Zucker *fa/fa* obese rat developed by Charles River Laboratory, Wilmington, MA, is a nondiabetic model of insulin resistance. These rats have marked obesity, hyperinsulinemia, insulin resistance, and mild hypertriglyceridemia. However, they are normotensive and normoglycemic. SD rats are normoglycemic with no insulin resistance.

First set of experiments. In the first set of experiments, EPCs from Zucker fatty rats and normal SD rats (n = 6 each) were obtained. Dose-dependant insulin stimulation of Akt phosphorylation (insulin signaling) was measured in Zucker and SD rat EPCs to compare the level of insulin resistance (Supplementary Fig. 1). Subsequently, the effect of TNF-α on insulin signaling and apoptosis was ascertained. The inhibitor of NF-κB, Bay-11, was used to determine whether these effects could be reversed in both Zucker and SD rats. In another set of experiments, EPCs from Zucker fatty rats (n = 6) were obtained and the effect of TNF-α on interleukin (IL)-8 secretion was assessed.

EPC culture and characterization. EPCs from Zucker fatty rats and SD rats were obtained in the following manner. Blood (7–8 mL) from insulin-resistant Zucker *fa/fa* obese or SD rats (14–15 weeks old) was obtained. Citrate-treated blood was centrifuged and treated with erythrocyte lysis buffer (ammonium acetate). Cells were counted and diluted to 5×10^6 cells/mL in sterile PBS with 5% BSA. Cells were then centrifuged to pellet cells. Primary antibodies (CD133-PE, eBioscience; CD34-PE-Cy7, Santa Cruz; and CD45-Alexa Fluor 647, Biolegend) were added to the cells and incubated with anti-mouse compensation beads (BD) for 30 min. Cells were then filtered through a cell strainer (BD Falcon). Cells were taken to the cell analysis facility and sorted on FACSAria (Becton-Dickinson) for cells that positively label for CD45, CD34, and CD133. Subsequently, cells were grown for 5 days on fibronectin-coated dishes in endothelial growth medium-2 (Lonza). Cells were then re-identified by incubating 100 μL of cells with the primary antibodies, taken to the cell-analysis facility, and resorted and analyzed by flow cytometry to check CD labeling after ex vivo expansion. Additionally, EPC characteristics were demonstrated by tube formation assay. Filtration was carried out to prevent cell clotting and microembolization.

Assessment of EPC IL-8 response to TNF-α. EPCs were serum starved for 10 h and then exposed to 10 ng/mL TNF-α for 12 h. Subsequently, media was collected and the assays for IL-8 (R&D Systems) were performed using enzyme-linked immunoassay (ELISA) kits per the manufacturer's protocols.

Assessment of EPC insulin signaling and survival in the presence/absence of TNF-α. EPCs, sorted as described above, were seeded onto a poly-L-lysine–coated 96-well plate and allowed to attach. The media was changed to starvation media (0.5% FBS in endothelial basal medium), and the cells were starved for 10 h. The cells were then treated with 10 ng/mL TNF-α and 3 μmol/L Bay11 for 12 h. Insulin (1 μmol/L) was then added for 1 h to stimulate the insulin signaling pathway. The cells were then assayed according to the directions of the cell-based ELISA (R&D Systems) for AKT and phosphorylated AKT (category no. KCB887). Briefly, the cells were treated with formaldehyde to fix the cells and then washed. The cells were then treated with quenching buffer, washed, treated with blocking buffer, and washed again. Subsequently, primary antibodies for phosphophorylated and total AKT were added and incubated overnight. The next day, the cells were washed and incubated with the secondary antibodies. The cells were washed, and substrate F1 was added. Later, substrate F2 was also added. The plate was read using a fluorescence plate reader at 600 nm (for phosphorylated AKT) and 450 nm (for total AKT). This was then expressed as a ratio.

EPC apoptosis. EPCs were sorted and prepared as described above. Cells were serum starved for 10 h and then treated with 10 ng/mL TNF-α and 3 μmol/L Bay11 for 12 h. The apoptosis assay was performed with Chemicon's Caspase-3 Colorimetric Activity Assay kit for assaying the activity of caspases that recognize the sequence Asp-Glu-Val-Asp (DEVD). After cleavage from the labeled substrate DEVD-pNA, the free pNA was quantified using a microtiter plate reader at 405 nm. We compared absorbance of pNA from apoptotic samples with that of uninduced controls, determining the fold increases in caspase-3 activity.

Angiogenesis tube formation elongation assay. Wells were coated with Extracellular Matrix gel (Category no. 10009964; Caymen Chemical Company) and allowed to solidify. EPCs were added to the gel with or without activators (25 or 50 μmol/L phorbol 12-myristate 13-acetate) or inhibitors (0.3 μmol/L; JNJ-10198409). Cells were placed in a cell culture incubator. After several days, calcein AM was added to the cells and the structure was captured using an inverted fluorescence microscope. Tube length was measured using analysis software. Results are shown in Supplementary Fig. 5.

Second set of experiments. EPCs from Zucker fatty rats (n = 6) were obtained sorted, expanded ex vivo as described earlier, and modified by suppressing NF-κB (RelA) with siRNA. The modified EPCs' response to TNF-α–induced IL-8 was assessed. The effect of TNF-α on insulin signaling and apoptosis in these modified EPCs was also ascertained.

Effect of NF-κB suppression: siRNA transfection. EPCs were sorted and cultured as described above. siRNA transfections were performed with Fugene 6 reagent according to the manufacturer's protocol. All three control siRNA (catalog no. 4611) and suppressor of cytokine signaling-3 or NF-κB siRNA (catalog no. AM16708A) were purchased from Ambion (Austin, TX). Briefly, a 24-well plate with 40,000 cells/well was exposed to 2 μL transfecting agent and siRNA at a concentration of 30 nmol/L for a period of 24 h. The medium was changed, and cells were treated with TNF-α (10 ng/mL) for 12 h. In the last hour, 10 nmol/L insulin was added. Subsequently, levels of AKT and phosphorylated AKT were measured and quantified as described earlier. There are three NF-κB (RelA) siRNA sequences in the kit. They are as follows: CCAUCAACUAUGAUGAGUUtt, CCGGAUUGAGGAGAAACGUtt, and GCCCAUGGAAUUCCAGUACtt.

RelA mRNA expression assessment: RT-PCR. Expression of NF-κB (RelA) mRNA was assessed by RT-PCR to gauge efficacy of silencing (25–27) as previously described. RNA was extracted using RNAwiz (Ambion, Austin, TX) and further purified using a Dnase treatment and removal kit (Ambion, Austin, TX). Gene-specific relative RT-PCR kits for rat NF-κB (Ambion) were used. Gene and species-specific sense and antisense primers as provided by the manufacturer were used. PCR products were resolved on an acrylamide gel, silver stained, and relatively quantified using 18S ribosomal RNA as endogenous control.

Assessment of RelA protein and modified EPCs. EPCs were cultured as described above, and RelA protein levels were measured using 10 nmol/L, 20 nmol/L, and 30 nmol/L concentrations of the RelA siRNA combination (ID1 and ID2). EPCs were transfected with RELA siRNA (Applied Biosystems). Cells were allowed to grow for 48 h. Cells were fixed with 4% formaldehyde and an in-cell Western assay was performed as per Li-Cor's instructions using RELA primary antibody (Cell Signaling) and DRAQ5 and Sapphire700 dyes (Li-Cor) for normalization. Protein levels of RelA are shown as percent of control levels. Modified EPCs were then assessed for TNF-α–induced IL-8 secretion and the effect of TNF-α on insulin signaling and apoptosis as described above.

Third set of experiments. In this experiment, all groups of Zucker fatty rats underwent carotid angioplasty as described below. There were four groups of rats with four rats in each group (total n = 16). Group 1 served as untreated controls. Group 2 rats were given unmodified Zucker rat CD45,133,34 EPCs (1×10^6 cells) postangioplasty intra-arterially. Group 3 rats were given Zucker rat CD45,133,34 EPCs (1×10^6 cells) modified to knockdown RelA with SureStep shRNA plasmids as described below (postangioplasty intra-arterially). For these three groups, carotids were harvested 3 weeks postangioplasty and neointimal hyperplasia was measured as described below. Group 4 rats were given modified Zucker rat CD45,133,34 EPCs, which were further labeled with the Qtracker system. The purpose of this group was to track and see whether modified EPCs were able to migrate, adhere, and proliferate in the injured areas of the carotid. The carotids for this group were harvested at 48 h (n = 2) and 1 week (n = 2) postangioplasty.

SureSilencing shRNA plasmid transfection: EPC modification. Zucker rat EPCs were obtained, expanded, and sorted as described above. They were then modified as follows. SureSilencing shRNA plasmids (SABiosciences) for NF-κB were used to ensure long-term stable transfection. One day before transfection, 8×10^6 cells were seeded in each well of a 24-well plate (for roughly 30–35% confluence) with 400 μL growth medium. On the day of transfection, 0.40 μg of each gene-specific shRNA plasmid and the negative control shRNA plasmid were added into separate 50-μL aliquots of Opti-MEM I Reduced-Serum Medium (Gibco). SureFECT (3.0 μL) was added to 50 μL Opti-MEM (7.5 μL SureFECT per microgram of plasmid) in each well. This was incubated for 10 min at room temperature. Then 50 μL of SureFECT was added to each 50 μL shRNA mix and incubated for 20 min at room temperature. Thereafter, each 100 μL mixture of shRNA and SureFECT was added to the appropriate well containing cells and 400 μL normal growth medium. Cells were incubated at 37°C in a CO_2 incubator for 24–48 h. Subsequently, the transfection efficiency as the number of transfected cells divided by the total number of cells was determined by RT-PCR as described above.

EPC labeling with Qtracker 800. Modified EPCs were rinsed with Hanks' balanced salt solution (Lonza) and then detached with trypsin (Lonza) and neutralized with TNS (Lonza). Cells were centrifuged to pellet cells and then resuspended and counted. Qtracker Component A and Component B (Invitrogen) were mixed in a 15-mL sterile conical tube and incubated for 5 min. Complete endothelial growth medium-2 (Lonza) was added to conical tubes and mixed. EPCs were added to the tubes and incubated at 37°C for 60 min. The cells were washed twice with sterile saline. Cells were visualized on the Odyssey (Li-cor) to check labeling of cells. Cells were held on ice until they were ready for injection.

Carotid angioplasty. Zucker *fa/fa* obese rats (age 14–15 weeks) were used. Angioplasty was done using a modified version of a method that has been used by us before (28,29). Rats were anesthetized with isoflourane, and the inner left thigh was shaved and cleaned. Under aseptic conditions, an incision was made to expose the left femoral artery. Homeostasis was achieved with an arterial clamp. A 2.3-F, 2-mm, balloon-length (20 mm) percutaneous transluminal coronary angioplasty catheter (Boston SCI-Med) was introduced into the femoral artery. The catheter was directed to the left carotid artery, with the help of a guide wire, under fluoroscopic guidance. Angioplasty was done at 4 atmospheres (atm), and then pressure was reduced to 2 atm and the balloon was dragged down the entire carotid from its bifurcation to the aortic arch as done in previous experiments. The balloon was then deflated. EPCs either unmodified or modified (1×10^6) were then given intra-arterially over 10 min, and the catheter removed. The femoral artery was ligated and homeostasis achieved. The wound was closed in three layers. Skin staples were used. Rats were under direct close observation for the next 30 min. All procedures were performed under a dissecting microscope and in the setting of a sterile vivarial operating room. When this procedure is used, neointimal thickness is detectable within 1 week and is extensive by 3 weeks.

Tissue retrieval. Rats were killed with carbon dioxide. Carotid arteries were perfused with formalin prior to removal. Through a midline cervical incision, both the left and the right carotid, from the aortic arch to the bifurcation, were removed and preserved in formalin.

Tracking of exogenously delivered modified EPCs. The rat carotids were perfused with PBS followed by 4% paraformaldehyde. The aortic arch and carotids were removed from the rat and put in paraformaldehyde and, later, 70% alcohol. The carotids were slit open and placed on a slide. The slide was scanned on the Odyssey (Li-cor) by scanning for the 800 nm fluorescence. The Qtracker 800 (Invitrogen) will fluoresce at 800 nm while the carotid will not fluoresce. The Qtracker is inherited for at least six generations of daughter cells, providing a relatively long-term retention in cells.

Localization of modified EPCs in the injured carotid. An injured carotid section was taken 1 week postangioplasty and DAPI, and Q-tracker 800 double staining was visualized under high resolution. DAPI dye was diluted 1:2,000, and tissues were exposed to the dye for 5 min. The tissues or cells were put on a slide and coverslip and viewed under a microscope. EPCs, double staining with Q-Tracker (red) and nuclear staining (blue), were visualized.

CD45,133,34 characterization of modified EPCs in vitro and in vivo. The rat modified primary EPCs were plated on poly-L-Lysine–coated slides and preserved with formalin. The cells were blocked with 5% BSA in PBS, and the appropriate primary antibodies—CD133, phycoethrin conjugated (eBioscience); CD133, phycoethrin-Cy7 conjugated (Santa Cruz); and CD45, AF647 conjugated (BioLegend)—were diluted and incubated with the cells. The cells were rinsed with PBS and mounted with Fluoromount-G (Southern Biotech). The samples were taken to the Confocal Laser Scanning Microscope Core Facility and analyzed on the Zeiss 510 Meta Confocal Laser Scanning Microscope using the 40× optic for the modified EPCs.

CD45,133,34 characterization of modified EPCs in vivo. Modified EPCs were given to Zucker rats postangioplasty as described above, and carotids were harvested at 48 h. The carotid was prepared and preserved with formalin and then blocked with 5% BSA in PBS, and the appropriate primary antibodies—CD133, phycoethrin conjugated (eBioscience); CD133, phycoethrin-Cy7 conjugated (Santa Cruz); and CD45, AF647 conjugated (BioLegend)—were diluted and incubated with the carotid. The cells were rinsed with PBS, and the carotid was mounted with Fluoromount-G (Southern Biotech). The samples were taken to the Confocal Laser Scanning Microscope Core Facility and analyzed on the Zeiss 510 Meta Confocal Laser Scanning Microscope using the 20× optic for the carotid.

Morphometric analysis: evaluation of neointimal hyperplasia. Morphometric analysis was done using a previously described method (28,29). The left carotid from the junction of the aortic arch to the junction of the bifurcation was taken. Formaldehyde-fixed carotids were embedded in paraffin. The carotid was sectioned into four equal parts. Four sections from the two middle parts at 3-mm intervals were used for analysis. The neoinitimal hyperplasia is maximal in the middle of the vessel as endothelial regrowth occurs from the aortic root and from the bifurcation and is last to regrow in this area. All four sections, as described above, were selected for measurements. Sections were stained with hematoxylin. Analysis on the stained sections was done with ×10 microscopic magnification. Computerized digital microscopic software (An@lysis) was used to obtain measurements of the intimal and medial areas by a previously described method (30). The I/M ratio was then obtained.

Statistical analysis. All statistical analysis were done using Prizm software (Graphpad, San Diego, CA). For the in vitro experiments, statistical analysis was performed on at least five independent observations in each experimental set by one-way ANOVA or Student t test according to the experimental design. If the overall ANOVA P value was significant, pairwise multiple comparisons were performed by a Student-Newman-Keuls test or the Tukey test. The results are expressed as means ± SEM. The threshold for statistical significance was set as $P < 0.05$.

For the animal experiments, the statistical data analysis was a two-way ANOVA, with factors being treatment (three groups). If ANOVA was significant, we followed up with a Tukey post hoc test to identify which subgroups were different. The overall level of significance was kept at 0.05.

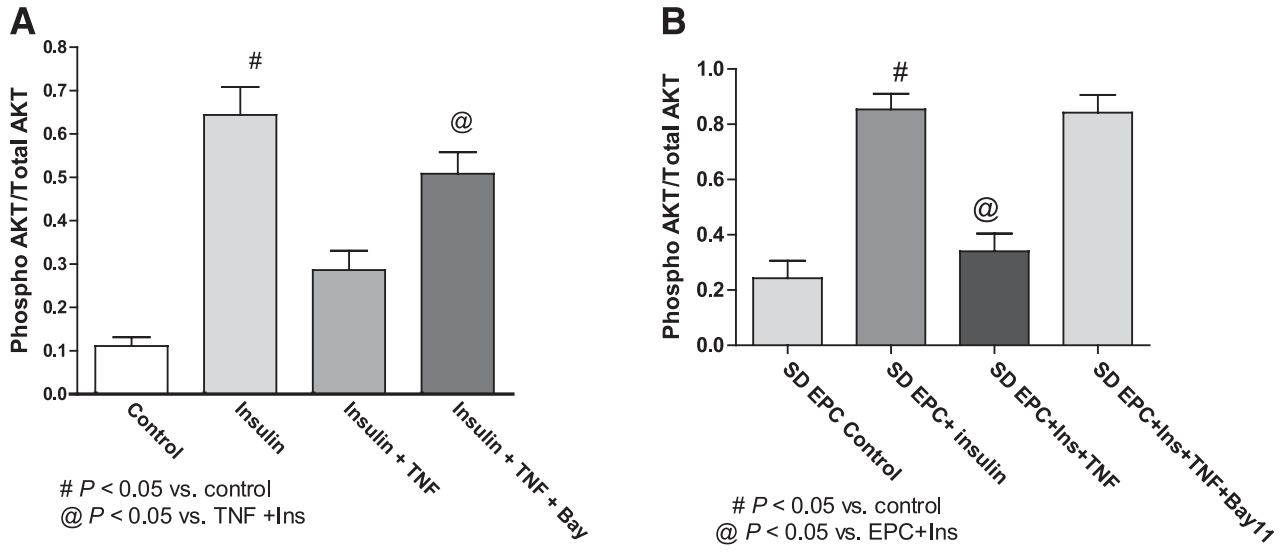

FIG. 1. *A*: Zucker rat EPCs exposed to TNF-α showed a marked 56% reduction in insulin (Ins)-stimulated AKT phosphorylation (phospho). Addition of NF-κB inhibitor BAY11 improved insulin-stimulated AKT phosphorylation in the presence of TNF-α to 80% of the insulin-stimulated AKT. *B*: SD rat EPCs exposed to TNF-α showed a marked 61% reduction in insulin-stimulated AKT phosphorylation. Addition of NF-κB inhibitor BAY11 improved insulin-stimulated AKT phosphorylation in the presence of TNF-α to 97% of the insulin-stimulated AKT.

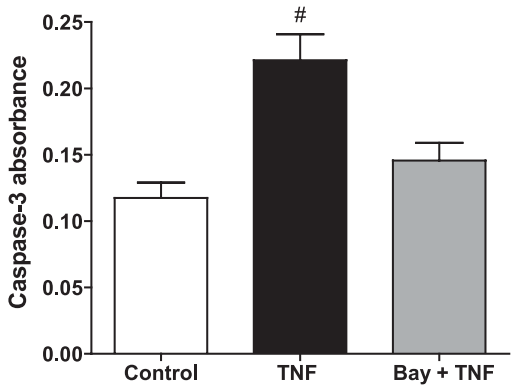

FIG. 2. Effect of TNF-α on apoptosis and reversal by NF-κB inhibitor BAY11 (Zucker rat EPCs). TNF-α increased apoptosis in EPCs significantly (71%) compared with controls. Addition of the NF-κB inhibitor BAY11 (BAY) decreased apoptosis down to control levels. #$P < 0.05$ vs. control and TNF-α plus BAY11.

RESULTS

First set of experiments

Insulin signaling. EPCs obtained from Zucker fatty rats were much more resistant to insulin as measured by Akt phosphorylation when compared with SD rats at various escalating doses of insulin. This suggests that EPCs from Zucker fatty rats are insulin resistant (Supplementary Fig. 1). EPCs obtained from Zucker Fatty rats were treated with different doses of TNF-α to obtain a dose-response curve for TNF-α–stimulated IL-8, and the ideal determined TNF-α dose was 10 ng/mL (Supplementary Fig. 2).

Zucker EPCs exposed to TNF-α showed a marked 56% reduction in insulin-stimulated AKT phosphorylation (Fig. 1*A*). Addition of NF-κB inhibitor BAY11 improved insulin-stimulated AKT phosphorylation in the presence of TNF-α to 80% of the insulin alone–stimulated AKT (Fig. 1*A*). SD rat EPCs exposed to TNF-α showed a marked 61% reduction in insulin-stimulated AKT phosphorylation (Fig. 1*B*). Addition of NF-κB inhibitor BAY11 improved insulin-stimulated AKT phosphorylation in the presence of TNF-α to 97% of the insulin-stimulated AKT (Fig. 1*B*). This suggests that insulin signaling in both Zucker and SD rat EPCs can be disrupted by cytokines and the inhibition of NFKB will reverse some of this signaling defect. In SD rat EPCs, the baseline stimulation of Akt is much higher than in Zucker EPCs. SD rat EPCs have a reduction in Akt phosphorylation similar to that of Zucker EPCs; however, BAY11, the NF-κB inhibitor, is fully able to reverse this defect in SD EPCs but only partially reverses it in Zucker EPCs.

Apoptosis. TNF-α increased apoptosis in EPCs significantly (71%) compared with controls. Addition of the NF-κB inhibitor BAY11 decreased apoptosis down to control levels (Fig. 2). Transferase-mediated dUTP nick-end labeling assay further confirmed this (Supplementary Fig. 4). Reduction of apoptosis could lead to increase survival time and, therefore, increased number of EPCs.

Second set of experiments

Reduction of NF-κB (RelA) mRNA expression in cultured Zucker EPCs. EPCs were transfected with siRNA initially for glyceraldehyde-3-phosphate dehydrogenase to verify whether EPCs are amenable to transfection as described in RESEARCH DESIGN AND METHODS. Glyceraldehyde-3-phosphate dehydrogenase expression was measured by

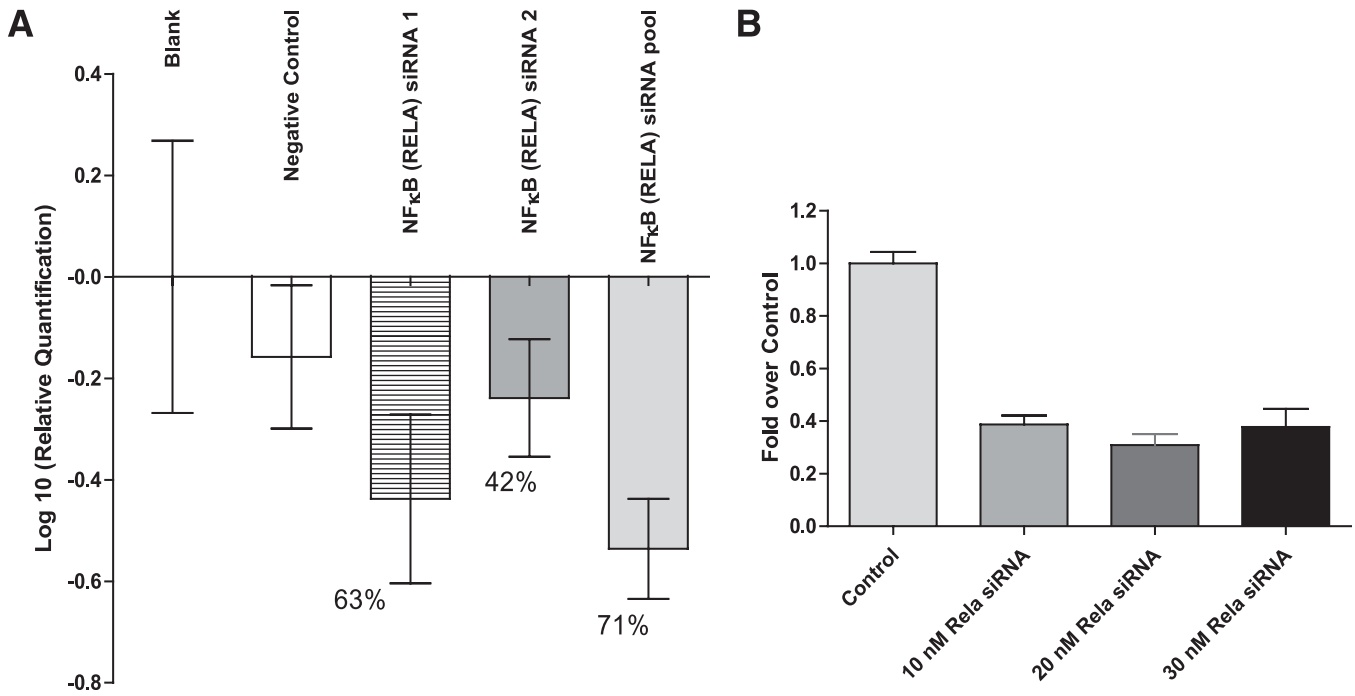

FIG. 3. *A*: siRNA knockdown of NF-κB. Each of the individual RelA siRNAs was able to decrease RelA mRNA expression as measured by RT-PCR. siRNA no. 1 had greatest effect, with a 63% decrease. siRNA no.3 was not effective (not shown). Combination of both RelA siRNAs resulted in a 71% reduction in NF-κB (RelA) mRNA expression. *B*: Protein knockdown of RelA using siRNA. RelA protein levels were measured using 10 nmol/L, 20 nmol/L, and 30 nmol/L concentrations of the RelA siRNA combination (ID1 and ID2). There was a 60, 70, and 59% decrease in RelA protein with the various concentrations, respectively, which matches the decreases seen in mRNA expression.

RT-PCR and showed significant reduction in expression (88%) (Supplementary Fig. 3).

EPCs were then transfected with three different siRNAs for RelA separately and in combination. These were obtained from Ambion, as described in RESEARCH DESIGN AND METHODS. Each of the individual RelA siRNAs was able to decrease RelA expression as measured by RT-PCR. siRNA no. 1 had greatest effect with a 63% decrease (Fig. 3). siRNA no.3 was not effective (not shown). Combination of both RelA siRNAs resulted in a 71% reduction in NF-κB (RelA) expression (Fig. 3*A*). This suggests that RelA mRNA expression is significantly reduced in these modified Zucker rat EPCs.

Reduction of NF-κB (RelA) protein in cultured Zucker EPCs. To further confirm that the decrease in RelA mRNA expression results in actual decrease in the RelA protein, in-cell Western measurements showed a 60, 70, and 59% decrease in RelA protein with the 10, 20, and 30 nmol/L concentrations, respectively, which matches the decreases seen in mRNA expression (Fig. 3*B*).

Suppression of TNF-α–stimulated IL-8 production in NF-κB (RelA) knockdown EPCs. EPCs in which RelA was suppressed as described above were exposed to 10 ng/mL TNF-α and compared with control nonaltered EPCs. The TNF-α–stimulated IL-8 production in the NF-κB suppressed cells was 46% less than that of the control nonsense siRNA EPCs (Fig. 4). This shows that RelA-suppressed EPCs are more resistant to an inflammatory stimulus such as TNF-α. These EPCs may therefore function better in an inflammatory environment.

Improved insulin signaling in TNF-α–exposed, NF-κB (RelA) knockdown EPCs. EPCs in which RelA was suppressed were exposed to 10 ng/mL TNF-α as described in RESEARCH DESIGN AND METHODS and compared with control nonaltered EPCs (Fig. 7). Modified EPCs exposed to TNF-α showed a lesser reduction (20%) in insulin-stimulated AKT phosphorylation versus a 55% reduction in unmodified EPCs (Fig. 5). This shows that insulin signaling is improved in RelA-suppressed EPCs compared with unmodified EPCs in an inflammatory environment. Improved insulin signaling could lead to better functioning and, hence, improved healing postangioplasty.

Decreased apoptosis in TNF-α–exposed NF-κB (RelA) knockdown EPCs. EPCs in which RelA was suppressed as described above were exposed to 10 ng/mL TNF-α and compared with control nonaltered EPCs (Fig. 6). Modified EPCs exposed to TNF-α showed a lesser degree of apoptosis compared with unmodified control EPCs (41% decrease for RelA knockdown) (Fig. 6).

Third set of experiments

Decreased neointimal hyperplasia postangioplasty in rats receiving modified EPCs. Zucker rats underwent carotid angioplasty as described in RESEARCH DESIGN AND METHODS. Three groups of rats were assessed for neointimal hyperplasia postangioplasty. Group 1 served as untreated controls, and group 2 rats were given unmodified Zucker rat CD45,133,34 EPCs (1×10^6 cells) postangioplasty intra-arterially. Group 3 rats were given Zucker rat CD45,133,34 EPCs (1×10^6 cells) modified to knockdown NF-κB with SureStep silencing RNA plasmids as described above: postangioplasty intra-arterially. Carotids were harvested 3 weeks postangioplasty.

There was a 32% reduction in carotid intimal hyperplasia in the Zucker rats treated with unmodified EPCs versus untreated controls (I/M ratio 1.02 vs. 1.62, respectively) (Fig. 7*A* and *B*). There was a 64% reduction in carotid intimal hyperplasia in Zucker rats treated with NF-κB–suppressed and modified EPCs versus that in untreated controls (I/M ratio 0.58 vs. 1.62, respectively) (Fig. 7*A* and *B*). These data clearly support the use of modified CD45,133,34 EPCs in reducing intimal hyperplasia.

The fourth group of rats also underwent angioplasty and received modified EPCs. However, they were killed at 48 h and 1 week to track the modified EPCs postangioplasty

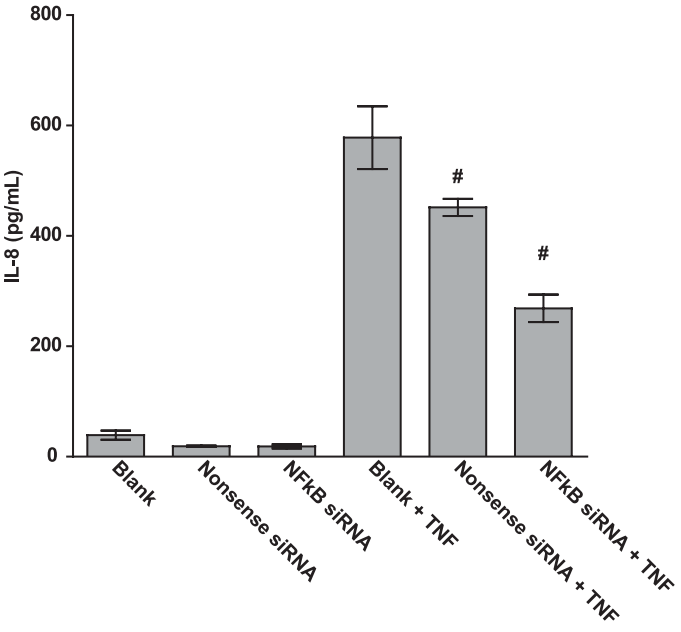

FIG. 4. Suppression of TNF-α–stimulated IL-8 production in NF-κB knockdown EPCs. Zucker rat EPCs, in which RelA was suppressed, were exposed to 10 ng/mL TNF-α and compared with control nonaltered EPCs. The TNF-α–stimulated IL-8 production in the NF-κB–suppressed cells was 46% less than that of the control nonsense siRNA EPCs. This shows that RelA-suppressed EPCs are more resistant to an inflammatory stimulus such as TNF-α. #$P < 0.05$ vs. nonsense siRNA and blank plus TNF.

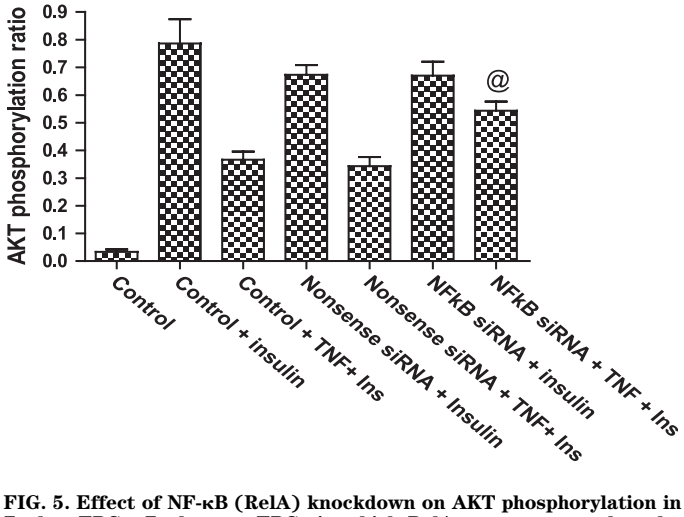

FIG. 5. Effect of NF-κB (RelA) knockdown on AKT phosphorylation in Zucker EPCs. Zucker rat EPCs in which RelA was suppressed as described above were exposed to 10 ng/mL TNF-α and compared with control nonaltered EPCs. Modified EPCs exposed to TNF-α showed a lesser reduction (20% decrease) in insulin (Ins)-stimulated AKT phosphorylation vs. a 55% reduction in unmodified EPCs. This shows that insulin signaling is improved in RelA-suppressed EPCs compared with unmodified EPCs in an inflammatory environment. @$P < 0.05$ vs. nonsense siRNA plus TNF plus insulin.

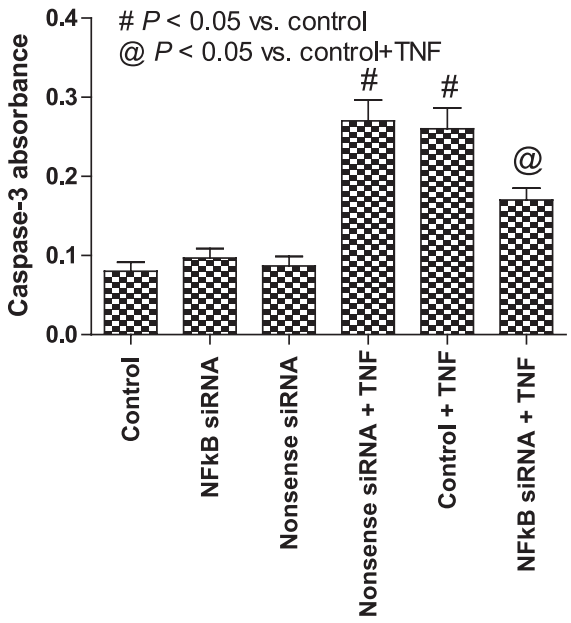

FIG. 6. Effect of RelA knockdown on apoptosis in Zucker fatty EPCs. Zucker rat EPCs in which RelA was suppressed were exposed to 10 ng/mL TNF-α and compared with control nonaltered EPCs. Modified EPCs exposed to TNF-α showed a lesser degree of apoptosis compared with unmodified EPCs (41% decrease for RelA knockdown).

using the Qtracker system. EPCs were detected adherent to the injured areas (red fluorescence) to a small extent 48 h later (Fig. 8*A*). EPCs proliferated and were more abundant 1 week later (Fig. 8*A*). An injured carotid section was taken 1 week postangioplasty, and DAPI and Q-tracker 800 double staining was visualized under high resolution. EPC double staining with Q-Tracker (red) and nuclear staining (blue) can be clearly seen (arrows) amid other cells with nuclear stain only (Fig. 8*B*). EPCs were further identified for CD 45,133,34 staining in vivo to ensure that EPCs had not yet changed characteristics (Fig. 8*C*).

EPCs can be characterized as early, late, or circulating depending on the CD markers identified. The question of which set of CD markers define which set of functional characteristics is still being sorted out. We refer the reader to an excellent review on this topic (31). This experiment shows that the modified EPCs can be tracked through initial cycles of proliferation at the site of vascular injury.

DISCUSSION

Several of the abnormalities associated with insulin resistance, including reduced nitric oxide (NO) bioavailability, increased production of reactive oxygen species, and downregulation of intracellular signaling pathways, have the potential to disrupt EPC function. Improvement in the number and function of EPCs may contribute to the protective actions of evidence-based therapies to reduce cardiometabolic risk (32). In this study, we show that EPCs from an insulin-resistant rat model, Zucker fatty rats, have impaired insulin signaling when exposed to an inflammatory stimulus. When EPCs from Zucker fatty rats were exposed to a cytokine, TNF-α, the insulin signaling defect as measured by AKT phosphorylation was worsened. EPCs also had increased apoptosis. By contrast, there is some evidence suggesting that NF-κB is involved in preventing TNF-α–induced apoptosis (12,33); however, in our study NF-κB suppression resulted in decreased apoptosis. In EPCs, the PI3K/Akt pathway has been implicated in the mobilization of EPCs from the bone marrow, EPC differentiation, and inhibition of EPC apoptosis.

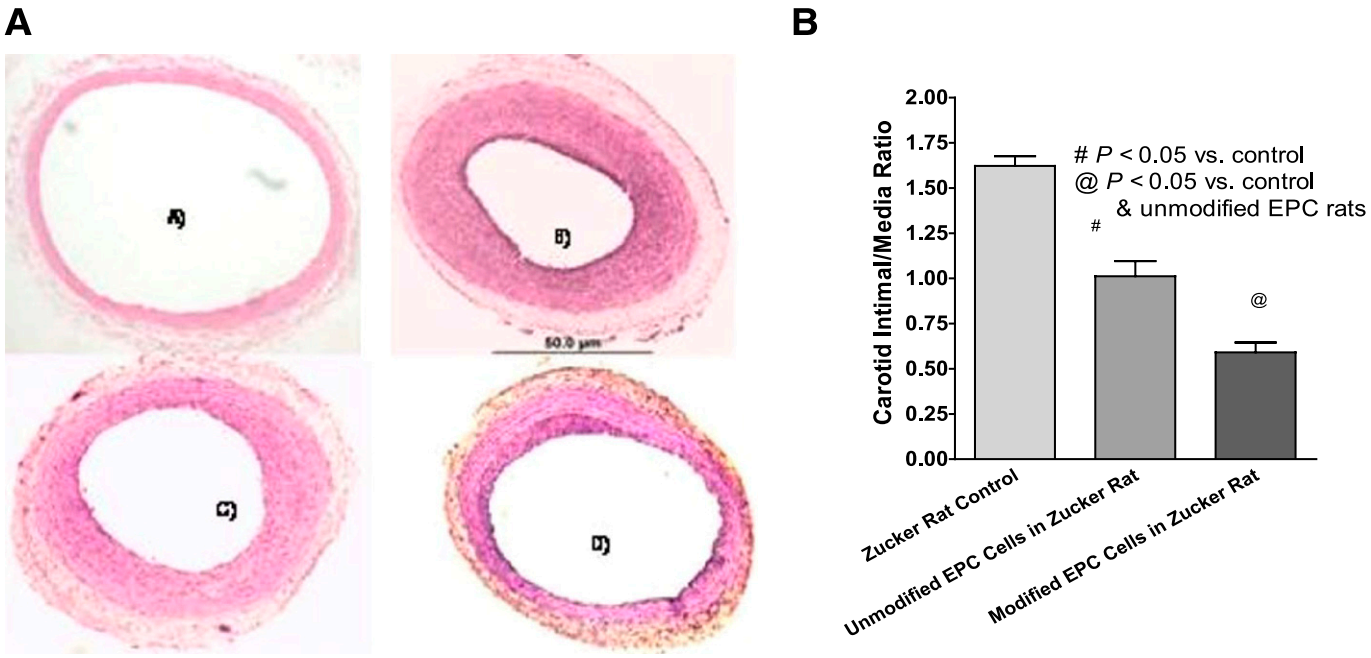

FIG. 7. *A*: Zucker fatty rat uninjured right carotid (*top left*), Zucker fatty rat untreated control injured carotid showing marked intimal hyperplasia (*top right*), Zucker fatty rat carotid treated with unmodified Zucker rat EPCs showing decreased carotid intimal hyperplasia (*bottom left*), and Zucker fatty rat carotid treated with modified Zucker rat EPCs showing markedly decreased carotid intimal hyperplasia (*bottom right*). *B*: Quantification of neointimal hyperplasia. There was a 64% reduction in carotid intimal hyperplasia in Zucker rats treated with NF-κB–suppressed modified EPCs vs. untreated controls (I/M ratio 0.58 vs. 1.62, respectively). (A high-quality color representation of this figure is available in the online issue.)

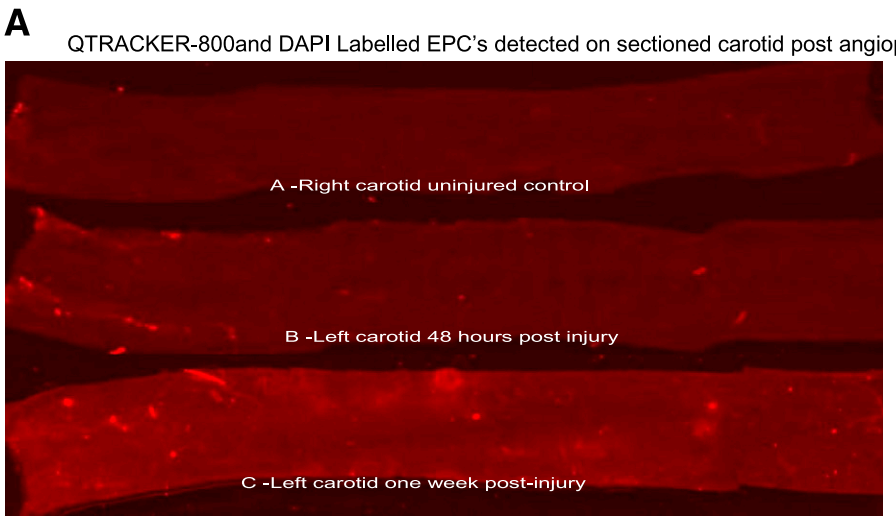

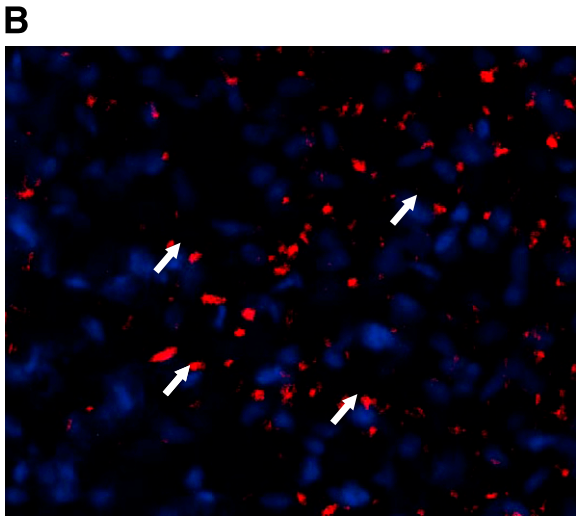

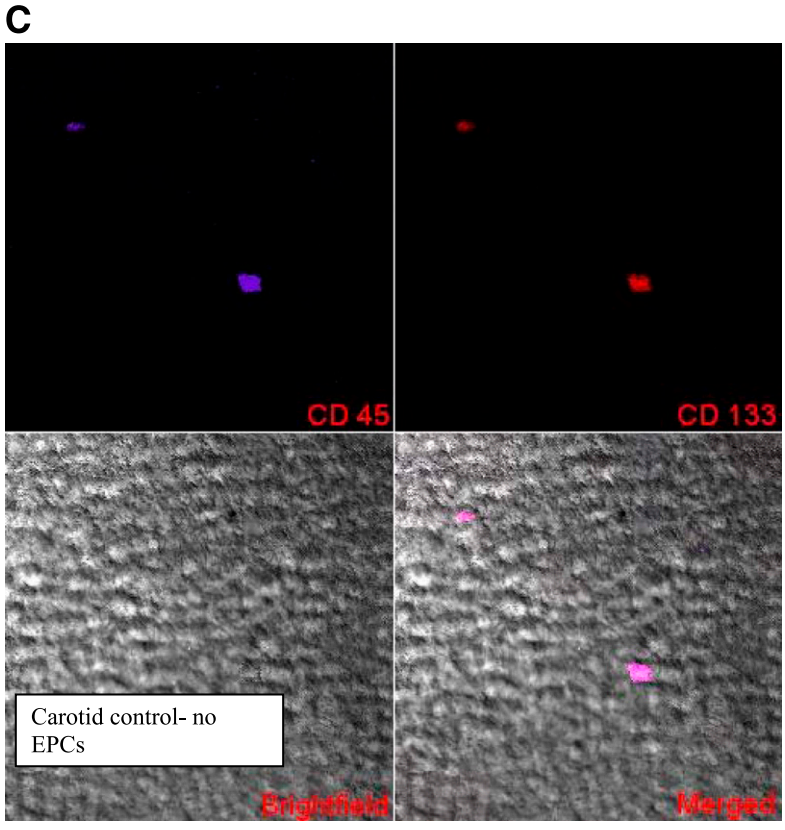

FIG. 8. ***A*****: Modified EPCs were labeled with Q-tracker 800 and given to rats just after angioplasty at the injury site as described in** RESEARCH DESIGN AND METHODS**. Carotids were harvested 48 h and 1 week later and visualized using Odyssey (Li-cor) to check labeling of cells.** ***A*****: The right carotid served as control (*****top*****), EPCs were detected adherent to the injured areas (red fluorescence) to a small extent 48 h later (*****center*****), and EPCs proliferated and were much more abundant 1 week later (*****bottom*****). This experiment shows that the modified EPCs can be tracked initially and after several cycles of proliferation at the site of vascular injury.** ***B*****: An injured carotid section was taken 1 week postangioplasty, and DAPI and Q-tracker 800 double staining were visualized under high resolution. EPCs double staining with Q-Tracker (red) and nuclear staining (blue) can be clearly seen (arrows) amid other cell with nuclear stain only.** ***C*****: An injured carotid section was taken out 48 h after angioplasty, and EPCs sating with CD45,133 were identified adherent to the carotid surface. (A high-quality digital representation of this figure is available in the online issue.)**

Inhibition of PI3K/Akt signaling abolishes EPC mobilization in response to statins and pioglitazone (34,35). Statins induce EPC differentiation via the PI3K/Akt pathway, as demonstrated by the inhibitory effect of selective pharmacological inhibitors (34). Genetic deletion of *Akt1* in mice results in impaired mobilization of EPCs in response to both ischemia and vascular endothelial growth factor (36). Downregulation of insulin signaling in insulin-resistant animals is selective for the PI3K/Akt pathway while signal transduction via the MAPK pathway is maintained (37). Selective abnormalities of PI3K/Akt signaling, therefore, may link insulin resistance with defective EPC survival, mobilization, proliferation, differentiation, and apoptosis. In this study, we have shown that inflammatory cytokines are likely to disrupt EPC insulin signaling and increase EPC apoptosis. Strategies that alleviate this disruption of

the insulin signaling pathway would likely lead to improved survival and function.

Some studies suggest that inhibitory effects on insulin signaling may be mediated by NF-κB, c-jun NH_2-terminal kinase, or MAPK pathways (38–41); hence, the inability of EPCs to respond adequately to insulin may result in dysfunction in the setting of insulin-resistant states. Moreover, insulin has potent anti-inflammatory effects that are greatly decreased as a result of the insulin resistance (42). This further increases inflammation, creating a pathological loop. We have demonstrated for the first time that inhibiting this pathological loop by knocking down NF-κB (RelA) and thus modifying Zucker rat EPCs can lead to improved insulin signaling and increased EPC survival.

Most importantly, improvement in EPC insulin signaling and survival should ultimately lead to improved vascular outcomes in in vivo models. In our model of vascular injury and restenosis in Zucker fatty rats, we show for the first time that EPCs modified by a knockdown of NF-κB (RelA), lead to decreased neointimal hyperplasia. Our study shows that increasing the number of EPCs in circulation is effective in decreasing neointimal hyperplasia postangioplasty. However, modifying EPCs so as to block the inflammatory stimulus leads to an even greater reduction in neointimal hyperplasia. EPCs resistant to cytokine stimulation would have improved insulin signaling and, hence, better function such as adhesion, migration, and proliferation, thus increasing the efficacy of reendothelialization and inhibition of vascular smooth muscle proliferation. We show in our study that these modified EPCs migrate and adhere to the injured areas of the blood vessel. It is possible that future studies show that they proliferate within the newly forming endothelium. Further studies need to be done to evaluate whether these modified EPCs stimulate more rapid endothelial regrowth or inhibit vascular smooth muscle proliferation.

In conclusion, we have shown that insulin signaling and EPC survival are impaired in Zucker fatty insulin-resistant rats. This defect can be ameliorated significantly by a knockdown of RelA. Modified EPCs then transfused into an insulin-resistant rat model reduce neointimal hyperplasia. The potential for translating this to humans would be very beneficial to patients who are at risk for cardiovascular disease in the setting of insulin resistance and inflammation.

ACKNOWLEDGMENTS

Part of this research was funded by a Veterans Affairs Merit Review grant. All of this work was done at the Omaha Veterans Affairs Medical Center. However, core facilities for sorting cells were at the University of Nebraska Medical Center.

No potential conflicts of interest relevant to this study were reported.

C.V.D. researched data, contributed to discussion, wrote the manuscript, and reviewed the manuscript. F.G.H. and K.B. contributed to discussion and edited the manuscript. K.O. researched data and contributed to discussion.

REFERENCES

1. Stern N, Izkhakov Y. The metabolic syndrome revisited: "cardiometabolic risk" emerges as common ground between differing views of the ADA and AHA. J Cardiometab Syndr 2006;1:362–363
2. Hong Y, Jin X, Mo J, et al. Metabolic syndrome, its preeminent clusters, incident coronary heart disease and all-cause mortality—results of prospective analysis for the Atherosclerosis Risk in Communities study. J Intern Med 2007;262:113–122
3. Sjöholm A, Nyström T. Endothelial inflammation in insulin resistance. Lancet 2005;365:610–612
4. Corros C, Jiménez-Quevedo P, Sabaté M. Diabetes mellitus and percutaneous coronary revascularization. Minerva Cardioangiol 2005;53:431–443
5. Berry C, Tardif JC, Bourassa MG. Coronary heart disease in patients with diabetes: part II: recent advances in coronary revascularization. J Am Coll Cardiol 2007;49:643–656
6. Diabetes, inflammation and cardiovascular disease. J Intern Med 2007;262:141
7. Ndumele CE, Pradhan AD, Ridker PM. Interrelationships between inflammation, C-reactive protein, and insulin resistance. J Cardiometab Syndr 2006;1:190–196
8. Shoelson SE, Herrero L, Naaz A. Obesity, inflammation, and insulin resistance. Gastroenterology 2007;132:2169–2180
9. Erol A. Insulin resistance is an evolutionarily conserved physiological mechanism at the cellular level for protection against increased oxidative stress. Bioessays 2007;29:811–818
10. Morisco C, Marrone C, Trimarco V, et al. Insulin resistance affects the cytoprotective effect of insulin in cardiomyocytes through an impairment of MAPK phosphatase-1 expression. Cardiovasc Res 2007;76:453–464
11. Kaneto H, Nakatani Y, Kawamori D, Miyatsuka T, Matsuoka TA. Involvement of oxidative stress and the JNK pathway in glucose toxicity. Rev Diabet Stud 2004;1:165–174
12. Liuwantara D, Elliot M, Smith MW, et al. Nuclear factor-kappaB regulates beta-cell death: a critical role for A20 in beta-cell protection. Diabetes 2006;55:2491–2501
13. Schiekofer S, Galasso G, Andrassy M, Aprahamian T, Schneider J, Rocnik E. Glucose control with insulin results in reduction of NF-kappaB-binding activity in mononuclear blood cells of patients with recently manifested type 1 diabetes. Diabetes Obes Metab 2006;8:473–482
14. Li G, Barrett EJ, Barrett MO, Cao W, Liu Z. Tumor necrosis factor-alpha induces insulin resistance in endothelial cells via a p38 mitogen-activated protein kinase-dependent pathway. Endocrinology 2007;148:3356–3363
15. Matsuda N, Yamamoto S, Yokoo H, Tobe K, Hattori Y. Nuclear factor-kappaB decoy oligodeoxynucleotides ameliorate impaired glucose tolerance and insulin resistance in mice with cecal ligation and puncture-induced sepsis. Crit Care Med 2009;37:2791–2799
16. Loomans CJ, de Koning EJ, Staal FJ, et al. Endothelial progenitor cell dysfunction: a novel concept in the pathogenesis of vascular complications of type 1 diabetes. Diabetes 2004;53:195–199
17. Michowitz Y, Goldstein E, Wexler D, Sheps D, Keren G, George J. Circulating endothelial progenitor cells and clinical outcome in patients with congestive heart failure. Heart 2007;93:1046–1050
18. Boos CJ, Lip GY, Blann AD. Circulating endothelial cells in cardiovascular disease. J Am Coll Cardiol 2006;48:1538–1547
19. Fadini GP, Sartore S, Schiavon M, et al. Diabetes impairs progenitor cell mobilisation after hindlimb ischaemia-reperfusion injury in rats. Diabetologia 2006;49:3075–3084
20. Fadini GP, Sartore S, Albiero M, et al. Number and function of endothelial progenitor cells as a marker of severity for diabetic vasculopathy. Arterioscler Thromb Vasc Biol 2006;26:2140–2146
21. Gallagher KA, Liu ZJ, Xiao M, et al. Diabetic impairments in NO-mediated endothelial progenitor cell mobilization and homing are reversed by hyperoxia and SDF-1 alpha. J Clin Invest 2007;117:1249–1259
22. Cubbon RM, Rajwani A, Wheatcroft SB. The impact of insulin resistance on endothelial function, progenitor cells and repair. Diab Vasc Dis Res 2007;4:103–111
23. Zhao X, Huang L, Yin Y, Fang Y, Zhou Y. Autologous endothelial progenitor cells transplantation promoting endothelial recovery in mice. Transpl Int 2007;20:712–721
24. Zhou B, Cao XC, Fang ZH, et al. Prevention of diabetic microangiopathy by prophylactic transplant of mobilized peripheral blood mononuclear cells. Acta Pharmacol Sin 2007;28:89–97
25. Bellezza I, Neuwirt H, Nemes C, et al. Suppressor of cytokine signaling-3 antagonizes cAMP effects on proliferation and apoptosis and is expressed in human prostate cancer. Am J Pathol 2006;169:2199–2208
26. Sands WA, Woolson HD, Milne GR, Rutherford C, Palmer TM. Exchange protein activated by cyclic AMP (Epac)-mediated induction of suppressor of cytokine signaling 3 (SOCS-3) in vascular endothelial cells. Mol Cell Biol 2006;26:6333–6346
27. Weigert C, Hennige AM, Lehmann R, et al. Direct cross-talk of interleukin-6 and insulin signal transduction via insulin receptor substrate-1 in skeletal muscle cells. J Biol Chem 2006;281:7060–7067

28. Indolfi C, Torella D, Coppola C, et al. Rat carotid artery dilation by PTCA balloon catheter induces neointima formation in presence of IEL rupture. Am J Physiol Heart Circ Physiol 2002;283:H760–H767
29. Desouza CV, Gerety M, Hamel FG. Neointimal hyperplasia and vascular endothelial growth factor expression are increased in normoglycemic, insulin resistant, obese fatty rats. Atherosclerosis 2006;184:283–289
30. Schiller NK, Timothy AM, Chen IL, et al. Endothelial cell regrowth and morphology after balloon catheter injury of alloxan-induced diabetic rabbits. Am J Physiol 1999;277:H740–H748
31. Steinmetz M, Nickenig G, Werner N. Endothelial-regenerating cells: an expanding universe. Hypertension 2010;55:593–599
32. Cubbon RM, Kahn MB, Wheatcroft SB. Effects of insulin resistance on endothelial progenitor cells and vascular repair. Clin Sci (Lond) 2009;117:173–190
33. Kast RE. Evidence of a mechanism by which etanercept increased TNF-alpha in multiple myeloma: new insights into the biology of TNF-alpha giving new treatment opportunities—the role of bupropion. Leuk Res 2005;29:1459–1463
34. Dimmeler S, Aicher A, Vasa M, et al. HMG-CoA reductase inhibitors (statins) increase endothelial progenitor cells via the PI 3-kinase/Akt pathway. J Clin Invest 2001;108:391–397
35. Werner C, Kamani CH, Gensch C, Böhm M, Laufs U. The peroxisome proliferator-activated receptor-gamma agonist pioglitazone increases number and function of endothelial progenitor cells in patients with coronary artery disease and normal glucose tolerance. Diabetes 2007;56:2609–2615
36. Ackah E, Yu J, Zoellner S, et al. Akt1/protein kinase Balpha is critical for ischemic and VEGF-mediated angiogenesis. J Clin Invest 2005;115:2119–2127
37. Jiang ZY, Lin YW, Clemont A, et al. Characterization of selective resistance to insulin signaling in the vasculature of obese Zucker (fa/fa) rats. J Clin Invest 1999;104:447–457
38. Gupta D, Varma S, Khandelwal RL. Long-term effects of tumor necrosis factor-alpha treatment on insulin signaling pathway in HepG2 cells and HepG2 cells overexpressing constitutively active Akt/PKB. J Cell Biochem 2007;100:593–607
39. Goren I, Müller E, Pfeilschifter J, Frank S. Severely impaired insulin signaling in chronic wounds of diabetic ob/ob mice: a potential role of tumor necrosis factor-alpha. Am J Pathol 2006;168:765–777
40. Medina EA, Afsari RR, Ravid T, Castillo SS, Erickson KL, Goldkorn T. Tumor necrosis factor-alpha decreases Akt protein levels in 3T3-L1 adipocytes via the caspase-dependent ubiquitination of Akt. Endocrinology 2005;146:2726–2735
41. Csehi SB, Mathieu S, Seifert U, et al. Tumor necrosis factor (TNF) interferes with insulin signaling through the p55 TNF receptor death domain. Biochem Biophys Res Commun 2005;329:397–405
42. Dandona P, Chaudhuri A, Mohanty P, Ghanim H. Anti-inflammatory effects of insulin. Curr Opin Clin Nutr Metab Care 2007;10:511–517